

SLOW INHIBITION OF Na⁺ CURRENT IN CRAYFISH AXONS BY 2-(1NON-8ENYL)-5-(1NON-8ENYL)PYRROLIDINE (Pyr9), A SYNTHETIC DERIVATIVE OF AN ANT VENOM ALKALOID

BRUNO LEBRUN¹ AND DANIEL CATTART^{2,*}

¹Laboratoire de Neurobiologie, Communication Chimique, LNB-CNRS, 31 Chemin J. Aiguier, 13402 Marseille, France and ²UPR Neurobiologie et Mouvements, NBM-CNRS, 31 Chemin J. Aiguier, 13402 Marseille, France

Accepted 19 May 1997

Summary

2,5-Dialkylpyrrolidines present in the venom of ants from the genus *Monomorium* are natural insecticides causing a flaccid paralysis. The mechanism of action of 2-(1non-8enyl)-5-(1non-8enyl)pyrrolidine (Pyr9), a synthetic derivative of 2,5-dialkylpyrrolidines, has been investigated *in vitro* on preparations of the ventral nerve cord of the crayfish *Procambarus clarkii*. Our results clearly indicate that Pyr9 blocks spike conduction without affecting the resting potential. Voltage-clamp experiments carried out on axons demonstrate that this blockade is due to a dual expression of Na⁺ current inhibition: a tonic inhibition developing slowly (90% of inhibition within 20 min for a Pyr9 concentration of 50 μmol l⁻¹) and independently of

stimulation, and a phasic inhibition developing during repetitive stimulation (5 Hz), the accumulation kinetics of which is 0.072 pulse⁻¹ at 5 Hz, according to the Courtney model. These findings suggest that tonic and phasic inhibition are due to different mechanisms. In addition, Pyr9 induces a shift of the Na⁺ inactivation curve towards more hyperpolarized potentials, which is in agreement with a higher affinity of Pyr9 for inactivated than for resting Na⁺ channels.

Key words: ant venom, pyrrolidine, Na⁺ channel inhibitor, local anaesthetic, crayfish, *Procambarus clarkii*.

Introduction

Ants of the genus *Monomorium* are natural predators of the termite genus *Reticulitermes*. They use a spatulated sting apparatus to apply small amounts of venom to the cuticle of their prey (Kugler, 1979; Jones *et al.* 1991). This venom induces paralysis within less than 1 min of topical application. Analysis of the venom of the genera *Monomorium* and *Solenopsis*, two taxa from the subfamily *Myrmicinae*, identified 2,5-dialkylpyrrolidines, 2,5-dialkylpyrrolines and 2-methyl-6-alkyl-piperidines as almost the only components (Blum *et al.* 1961, 1973, 1985; Brand *et al.* 1972; MacConnell *et al.* 1970; Pedder *et al.* 1976; Jones *et al.* 1982, 1988). The insecticidal activity of dialkylpyrrolidines has been documented experimentally (Clément *et al.* 1985*a,b*; Escoubas and Blum, 1990). None of the diverse pharmacological effects reported up to now, e.g. repellence of a variety of ants (for a review, see Jones and Blum, 1983) and vasodilatory activity (Gessner *et al.* 1987), can account for the rapid paralysis of treated insects.

Our preliminary studies indicated that dialkylpyrrolidines act by inhibiting Na⁺ currents involved in nerve conduction (Cattaert and Lebrun, 1993). In the present *in vitro* study, we investigated the mechanisms by which dialkylpyrrolidines

block action potentials in preparations of the ventral nerve cord of the crayfish *Procambarus clarkii*.

Materials and methods

A *cis-trans* diastereomeric mixture of Pyr9 synthesized according to Jones *et al.* (1982) was supplied by Professor G. Lhomme (Université P. et M. Curie, Paris, France). As Pyr9 is highly hydrophobic, we first studied its effect on nerve conduction when applied to nervous tissue *via* a lipophilic pathway: Pyr9 was diluted in paraffin oil whilst stirring and gently warming (at approximately 40 °C), and applied on a lipophilic interface as described below. An aqueous dispersion of Pyr9 was also perfused on *in vitro* nervous tissue preparations. The test perfusate was obtained by adding a small amount of Pyr9, previously diluted in ethanol, to normal saline and stirring overnight to obtain a fine clear emulsion. The final concentration of ethanol in the aqueous dispersion was less than 0.1% (v/v) and had no effect on Na⁺ currents.

Two types of *in vitro* preparations of the ventral nerve cord from the crayfish *Procambarus clarkii* Girard were used. The first was designed to study the effect of Pyr9 on nerve conduction. It

*Author for correspondence (e-mail: cattaert@lnc.cnrs-mrs.fr).

consisted of the three last thoracic ganglia, together with the motor nerves from the fifth thoracic ganglion to the proximal muscles. The thoracic nerve cord was pinned dorsal side up to a Sylgard-lined Petri dish, and the fourth and fifth thoracic ganglia were desheathed to improve perfusion of central neurones and to allow intracellular recordings from motoneurons. Intracellular recordings and stimulations of motoneurons were performed with glass micropipettes filled with KCl (3 mol l^{-1} ; resistance $10\text{--}20 \text{ M}\Omega$). Extracellular recordings from motor nerves were performed with *en passant* platinum wire electrodes and were differentially amplified (differential a.c. amplifier, model 1700 from AM-Systems, Inc., USA). A Vaseline well was built on the peripheral end of the motor nerve containing the axon of the motoneurone from which intracellular recordings were being made. Pyr9 was either deposited in this well as a paraffin oil solution or perfused as an aqueous dispersion.

The second type of *in vitro* preparation was designed to allow voltage-clamping of axons (Cattaert and Lebrun, 1993) to study the ionic currents affected during conduction blockade. The ventral nerve cord from the fourth thoracic ganglion to the first abdominal ganglion was isolated and pinned dorsal side up to a Sylgard-lined Petri dish (diameter 4 cm). The connective between the fifth thoracic ganglion and the first abdominal ganglion was desheathed. To restrict the range of the clamp to a short segment of axon, a 1–3 mm length of the desheathed nerve cord was mechanically isolated by squeezing it with wire staples pinned to the Sylgard. A double-electrode voltage-clamp was then performed on a restricted axon.

In these voltage-clamp experiments, glass micropipettes were filled with either 3 mol l^{-1} KCl or 1 mol l^{-1} tetraethylammonium chloride hydrate (TEA-Cl) and had a resistance of $2\text{--}6 \text{ M}\Omega$. A voltage-clamp amplifier (Axoclamp 2A; Axon Instruments) was used in either the bridge or the two-electrode voltage-clamp mode, with probes of $\times 0.1$ (for voltage) and either $\times 1$ or $\times 10$ (for current). Command pulses were controlled by a programmable stimulator (Master 8; AMPI, Israel).

The bathing solution was either normal saline (in mmol l^{-1} : 195 NaCl, 5.5 KCl, 13.5 CaCl_2 , 2.5 MgCl_2 and 10 Tris at pH 7.6) or saline containing TEA-Cl (10 mmol l^{-1}) and 4-aminopyridine (4-AP) (1 mmol l^{-1}). In some experiments, the Na^+ channel blocker tetrodotoxin (TTX, $10^{-6} \text{ mol l}^{-1}$) was added to the saline. The preparation was maintained at 9°C (unless otherwise noted) by a Peltier effect cooler (Sqalli-Houssaini *et al.* 1991). All chemicals used (TTX, TEA⁺ and 4-AP) were purchased from Sigma.

Data were stored on a digital tape recorder (Biologic DTR 1800) and displayed on a four-channel digital oscilloscope (Yokogawa). Data acquisition and analysis were controlled by a PCA 20 Tandon computer connected to an analog/digital interface (CED 1401; Cambridge Electronic Device) using a SIGAV program from CED that allows superimposition and averaging of triggered voltage and current traces.

Theoretical curves were fitted to the data using a least-squares algorithm (Prism; GraphPad Software, Inc, USA). In order to test the significance of the effect of Pyr9 on the Na^+

current inactivation curve, comparisons of best-fit values of parameters (V_{50} and slope factor, see text) in a series of control and treated preparations (Figs 5D, 6D) were performed using a paired *t*-test. The same procedure was used to compare the results shown in Fig. 8.

Results

Effects of Pyr9 on nerve conduction

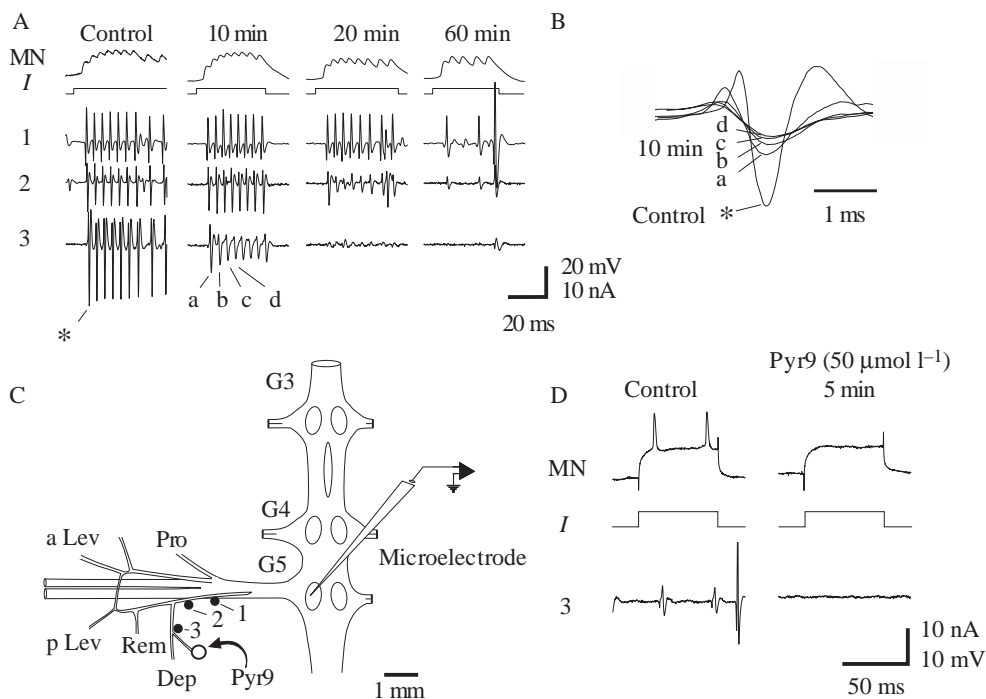
We analyzed the effects of Pyr9 on nerve conduction using the first type of *in vitro* nerve preparation described above. The orthodromic propagation of action potentials elicited by intracellular stimulation of a depressor motoneurone was recorded from the depressor motor nerve by three extracellular electrodes at several locations along the nerve (Fig. 1C). Spontaneous activity in other motor nerves was recorded extracellularly. The recordings obtained in control conditions (Fig. 1A) showed that the intracellularly evoked spikes were recorded from all three *en passant* electrodes, with different delays because of the conduction velocity.

Local application of Pyr9 as a paraffin oil solution ($10^{-3} \text{ mol l}^{-1}$) in a Vaseline well built at the peripheral end of the depressor nerve (open circle in Fig. 1C) led to a blockade of spike conduction in this nerve, without affecting spontaneous activity recorded from other nerves (not shown). This blockade appeared progressively along the nerve, according to the distance between the site of application of Pyr9 and the position of the recording electrode (Fig. 1A,C). Ten minutes after application of Pyr9, the amplitude of the spikes recorded from electrode 3 (closest to the Pyr9 application site) was reduced by 50% compared with the control. No change was observed in the spikes recorded from electrodes 2 and 1. Twenty minutes after treatment, the amplitude of spikes was reduced by 97% at electrode 3 and by 28% at electrode 2. After 1 h, the spikes recorded from electrode 1 were also affected by Pyr9. The blocking effect apparently propagated along the nerve at a velocity of approximately $2\text{--}5 \text{ mm h}^{-1}$.

In addition, Pyr9 seemed to block action potentials in at least two different ways. (i) A tonic block that appears as a progressive decrease of the spike amplitude, which can be estimated by comparing the amplitude of the first spike of a train of spikes under control condition with that after Pyr9 application (trace a) (Fig. 1A,B). Thus, after 10 min of Pyr9 application, the tonic block was estimated to be 50%. (ii) A phasic block characterized by a decrease in the spike amplitude during a train of spikes. The first spike is the largest of the train, and each following spike is smaller than the preceding one (a plateau is generally reached after the fourth spike which is, therefore, the smallest in the train). In Fig. 1A,B, the successive spikes of a train of spikes recorded from electrode 3 have been labelled a–d; after 10 min of exposure to Pyr9, the reduction in spike amplitude between spikes a and d corresponds to a phasic block of 37%.

Up to 1 h after treatment, the resting potential of the motoneurone was unaffected and spikes could still be elicited

Fig. 1. Effects of Pyr9 on the orthodromic propagation of spikes in crayfish nerves. (A) Recordings of the orthodromic propagation of intracellularly evoked spikes from a depressor motoneurone. MN, intracellular recording from a depressor motoneurone during injection of depolarizing current (*I*) pulses; 1, 2 and 3, extracellular recordings of orthodromically propagated spikes at three locations along the depressor nerve in control conditions and after exposure for different durations to locally applied Pyr9. (B) Superimposed spike recordings obtained at *en passant* electrode number 3 in control conditions (*) and the first four spikes of a train obtained 10 min after application of Pyr9 (a, b, c and d) (see A). (C) Diagram of the *in vitro* nerve preparation from the crayfish *Procambarus clarkii* consisting of the last three thoracic ganglia (G3, G4 and



G5) together with the motor nerves from the fifth thoracic ganglion to the proximal muscles of a locomotor appendage. The locations of the *en passant* platinum wire electrodes are shown (filled circles) as well as the site of topical application of Pyr9 through a lipophilic interface (an open circle). Pro, Rem, a Lev, p Lev, Dep, motor nerves innervating promotor, remotor, anterior levator, posterior levator and depressor muscles, respectively. (D) Pyr9 application as an aqueous dispersion in the bath blocks nerve conduction. Under control conditions, a pulse of depolarizing current (*I*) injected intracellularly into a depressor motoneurone (MN) evokes spikes that are conveyed in the depressor nerve and recorded *en passant* at site 3. After 5 min of exposure to 50 μmol l⁻¹ Pyr9, the same depolarizing pulse is unable to elicit a spike.

intracellularly, although they could not be propagated orthodromically along the nerve.

However, Pyr9 had a differential effect on the motor fibres in the depressor nerve. One hour after Pyr9 application, the intracellularly evoked spikes could not reach electrode 3, whereas a spike from a different unit could be propagated along the depressor nerve (Fig. 1A). Nevertheless, this large-amplitude unit (see recording from electrode 1) was dramatically reduced at electrode 3, suggesting that it was also partly blocked by Pyr9. In the same preparation, when Pyr9 (10⁻⁴ mol l⁻¹) was applied by superfusion, the conduction of the action potential was blocked in all the recorded nerves (data not shown).

When Pyr9 was applied as an aqueous dispersion in the bath (50 μmol l⁻¹), it usually blocked all activity in all motor nerves within less than 10 min. In the experiment presented in Fig. 1D, a depressor motoneurone produced spikes in response to a pulse of depolarizing current injected into the neurite within the ganglion. Each spike was actively conveyed along the motor nerve and recorded at site 3 in the depressor nerve. After bath application of Pyr9 (50 μmol l⁻¹), no spike could be evoked in this depressor motoneurone and all activity disappeared in the other motor nerves.

Effects of Pyr9 on resting potential

No significant effect on resting potential could be observed, even after long exposures at high concentrations

(>1 h, 5 × 10⁻⁵ mol l⁻¹ Pyr9), as shown in Table 1. The difference between the resting potential under control

Table 1. Effect of Pyr9 on resting potential

	Resting potential (mV)		
	Control	Pyr9	Difference
	-78	-80	-2
	-72	-73	-1
	-66	-67	-1
	-66	-67	-1
	-70	-70	0
	-67	-67	0
	-72	-72	0
	-68	-68	0
	-77	-76	1
	-67	-66	1
	-67	-65	2
	-63	-62	1
	-62	-62	0
	-65	-62	3
	-70	-69	1
	-71	-68	3
	-52	-52	0
Mean	-67.82	-67.41	0.41
S.D.	5.95	6.27	1.37

conditions and that after bath application of Pyr9 was 0.41 ± 1.37 mV (mean \pm s.d.; $N=17$).

Effects of dialkylpyrrolidines on inward current

The effect of Pyr9 on Na^+ current (I_{Na}) was determined using the two-electrode voltage-clamp technique on axons of abdominal flexor motoneurons.

Depolarization of axons from -70 mV to -30 mV or more evoked transient inward currents that inactivated within a few milliseconds. These currents were blocked by tetrodotoxin (10^{-6} mol l^{-1}) (Fig. 2A) and reversed around the Na^+ equilibrium potential (Fig. 2B,C), thus indicating that they result from activation of voltage-gated Na^+ channels.

Tonic inhibition of I_{Na}

Before application of Pyr9, the inward current elicited by 10 ms depolarizing pulses (-20 mV) from a holding potential of -80 mV was stable in amplitude (Fig. 3). In the absence of Pyr9, these Na^+ currents could be recorded for up to 1 h

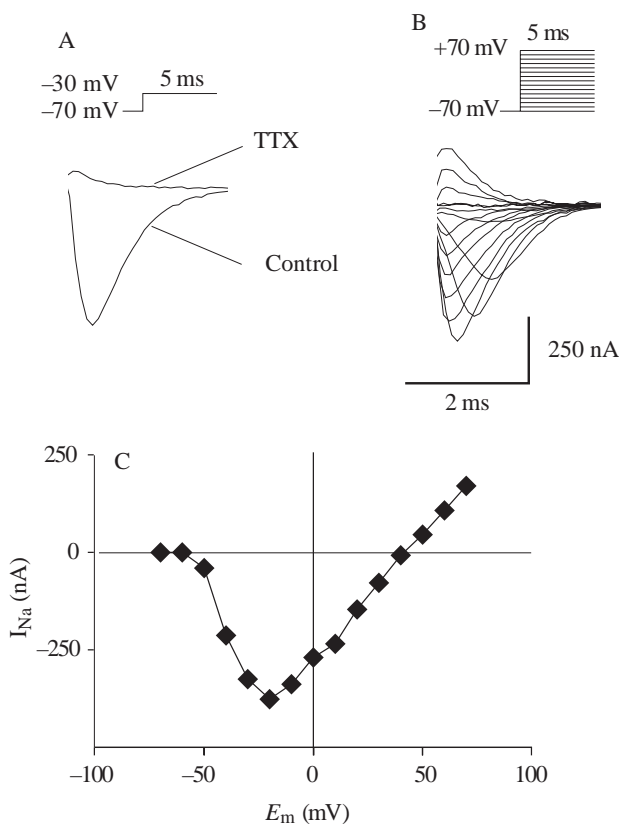


Fig. 2. A representative recording of the Na^+ current (I_{Na}) from a two-electrode voltage-clamped crayfish axon. (A) Superimposed current traces obtained under control conditions and after application of tetrodotoxin (TTX, 10^{-6} mol l^{-1}) by a pulse depolarization (-30 mV) from the holding potential (-70 mV). Total currents are shown, without subtraction of leak and capacitive currents. (B) Na^+ currents obtained at several depolarizing potentials after subtraction of the total currents recorded in the presence of TTX (10^{-6} mol l^{-1}). (C) Na^+ current amplitude as a function of pulse test potential (E_m) (results from a single experiment).

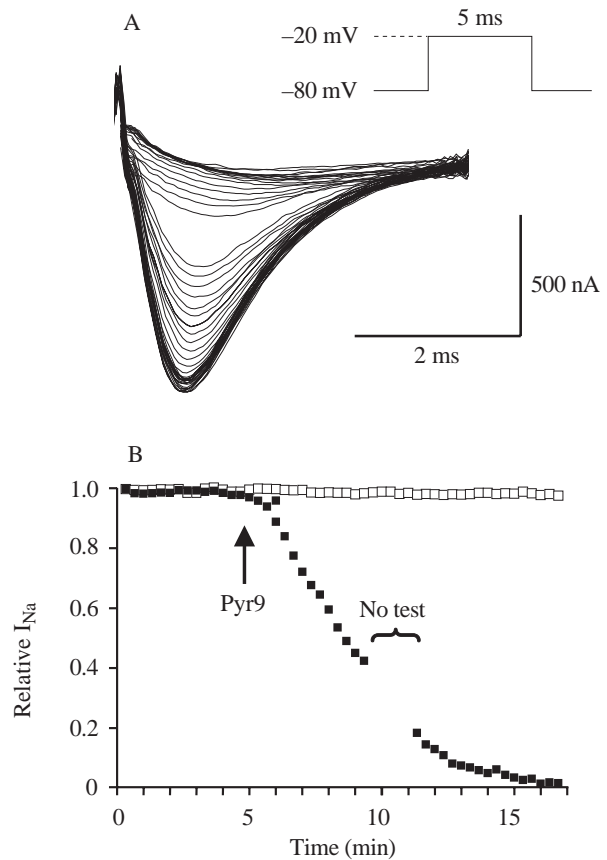


Fig. 3. Tonic inhibition of Na^+ current by Pyr9 ($50 \mu\text{mol l}^{-1}$). (A) Superimposed total current traces obtained by depolarizing pulses (-20 mV; 5 ms) applied at a frequency of 0.05 Hz under control conditions (the first 14 stimulations) and in the presence of $50 \mu\text{mol l}^{-1}$ Pyr9 (leak and capacitive currents were not subtracted). (B) Relative I_{Na} measured from the current traces presented in A as a function of time. Each point was normalized to the maximum Na^+ current amplitude. The arrow on the graph shows the beginning of Pyr9 perfusion (filled squares). When 60% of I_{Na} was inhibited, the stimulation was interrupted for 2 min (No test). However, this interruption did not change the progress of Pyr9 inhibition. Open squares, control experiment without Pyr9.

without noticeable changes (Fig. 3B, open squares). Application of Pyr9 ($50 \mu\text{mol l}^{-1}$) slowly reduced the amplitude of Na^+ current evoked by depolarizing pulses (0.05 Hz) to less than 40% of its initial amplitude within 10 min (Fig. 3B, filled squares) and caused more or less total inhibition within 20 min. After such a long exposure to Pyr9, the inhibition could not be reversed, even by 30 min of perfusion with a drug-free medium. The same protocol was used in nine experiments; in all cases, the Na^+ currents observed 20 min after $50 \mu\text{mol l}^{-1}$ Pyr9 application were reduced by between 50% and 100% (mean 80%). This variability is probably due to the hydrophobic nature of Pyr9, which made it impossible to ascertain its real aqueous concentration and thus prevented the production of a dose-response curve.

Phasic inhibition of I_{Na}

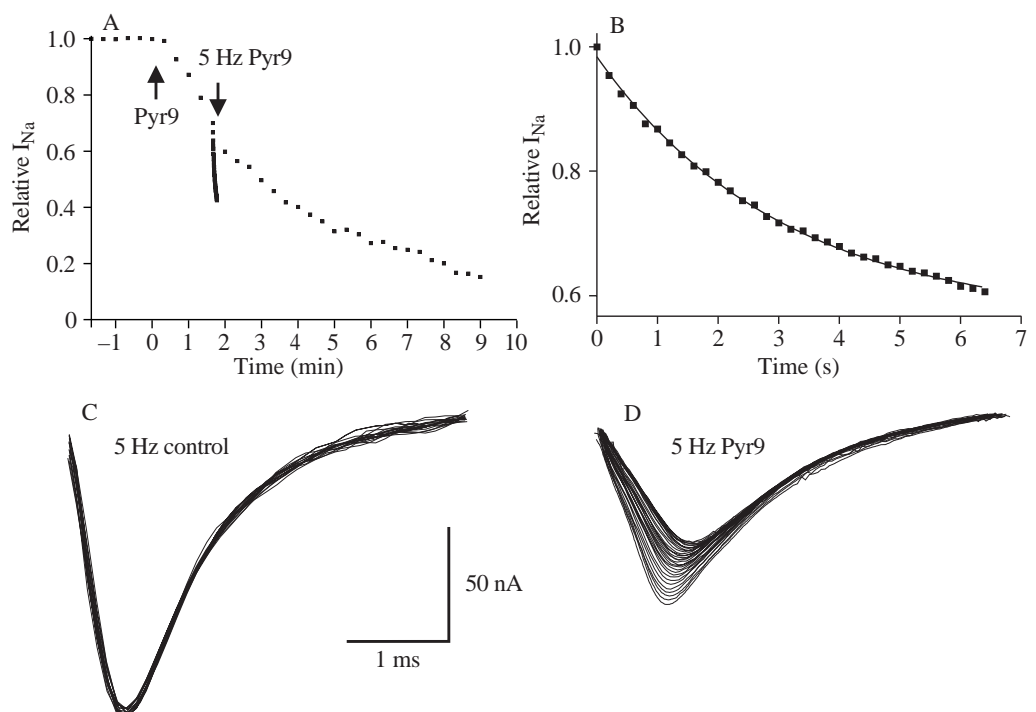
In addition to this tonic inhibition, Pyr9 also inhibited the Na⁺ current in a frequency-dependent manner. In the experiment illustrated in Fig. 4, treatment with Pyr9 (50 μmol l⁻¹) produced a tonic inhibition of 80% in 10 min at a low stimulation frequency (0.05 Hz). An additional inhibition was observed when the frequency of the applied stimuli was increased to 5 Hz. This was readily reversed when the stimulation frequency was lowered again (Fig. 4A). At the end of a train of 32 pulses, the phasic inhibition had reduced the relative I_{Na} by approximately 40% (Fig. 4B). The Na⁺ current amplitude is an exponential function of time during the phasic inhibition, as shown by the fitting of data points in Fig. 4B to the equation:

$$\text{Relative } I_{\text{Na}} = A_1 e^{-t/\tau_1} + C, \quad (1)$$

where A_1 is the steady-state relative inhibition value of Na⁺ current, C is the relative steady-state value of Na⁺ current, t is time and τ_1 is the time constant for the decline of Na⁺ current amplitude. The fit of the data points shown in Fig. 4B according to equation 1 gives $A_1 = 0.3969 \pm 0.0008$, $C = 0.579 \pm 0.013$ and $\tau_1 = 2.77 \pm 0.23$ s (95% confidence interval, CI; $r^2 = 0.996$).

The phasic inhibition was tested in different experiments at various degrees of tonic inhibition with Pyr9. The phasic inhibition at 5 Hz initiated when more than 65% of the Na⁺ current was already inhibited by Pyr9 ($A_1 = 0.334 \pm 0.009$, $C = 0.655 \pm 0.010$, $\tau_1 = 2.57 \pm 0.21$ s; $r^2 = 0.996$) was not significantly different from that initiated at the beginning of the inhibition (t -test applied to τ_1 ; $P = 0.207$).

Fig. 4. Tonic and phasic inhibition of Na⁺ current by Pyr9 treatment. (A) Relative Na⁺ current amplitude as a function of time. Each point was normalized to the maximum Na⁺ current amplitude. The upward arrow indicates the beginning of perfusion by Pyr9 (50 μmol l⁻¹). The protocol of stimulation consisted of a depolarizing step (-30 mV; 10 ms) applied at a low frequency (0.05 Hz) from a holding potential of -70 mV. The downward arrow indicates a 32-pulse train given at a frequency of 5 Hz (shown in B with a faster time scale). After this 5 Hz episode, the first protocol (0.05 Hz) was applied again. (B) Relative Na⁺ current obtained at a frequency of stimulation of 5 Hz as a function of time of stimulation. Each point was normalized to the Na⁺ current amplitude at the beginning of the 5 Hz episode. The smooth curve through the data is fitted according to equation 1. (C,D) Superimposed current traces obtained with 5 Hz stimulation under control conditions (C) and in the presence of Pyr9 (D).



In these experiments, stimulation at 5 Hz did not evoke any reduction in Na⁺ current under control conditions (Fig. 4C) and, therefore, it can be concluded that the phasic inhibition is a phenomenon induced by Pyr9 application (Fig. 4D).

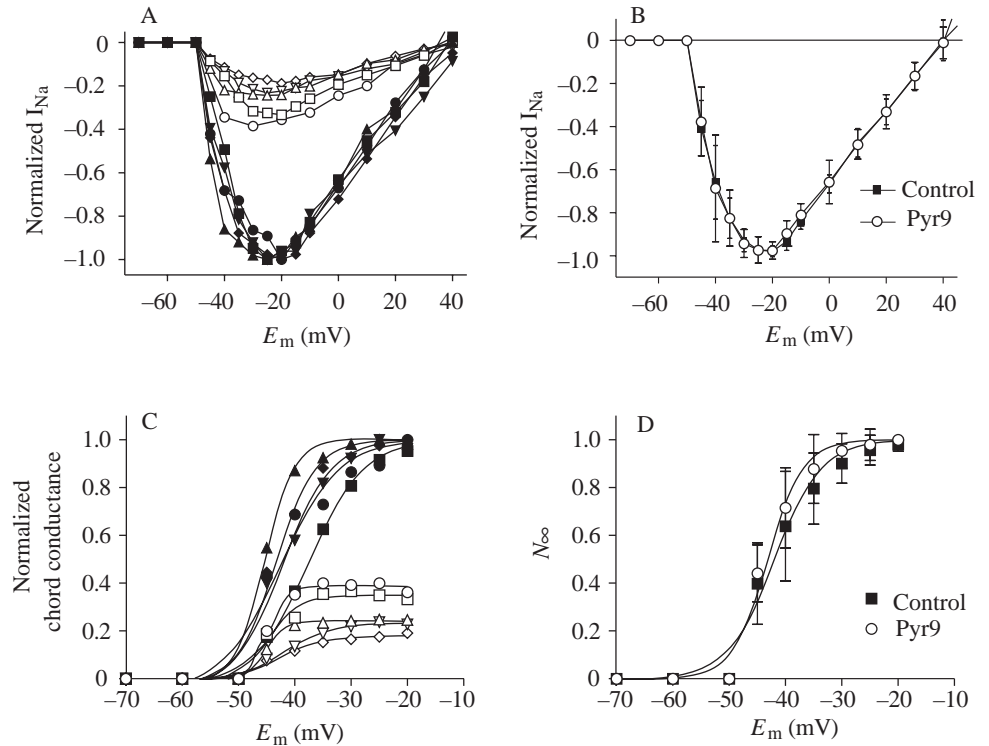
Effect of Pyr9 on the Na⁺ current activation curve

The effect of Pyr9 on the Na⁺ current activation curve is presented in Fig. 5. The holding potential was set to -70 mV, and peak inward current responses to various step depolarizations (5 ms; from -60 mV to 40 mV) were measured (Fig. 5A). Data from five abdominal flexor motoneurons have been normalized to the maximum value obtained for each motoneuron under control condition. In the presence of Pyr9 (50 μmol l⁻¹), only the amplitude of the curves appeared to be affected. Averaged responses normalized to the maximum peak amplitude obtained for each curve are presented in Fig. 5B (mean ± 95% CI). There is no significant difference between these two curves. From these values of peak inward current, the activation curves were calculated using the following equation:

$$G = I \times (V_m - E_R), \quad (2)$$

where G is the chord conductance associated with the peak of the inward current I , E_R is the equilibrium potential for Na⁺ and V_m is the test potential. These values have been normalized to the maximum conductance obtained for each motoneuron under control conditions (Fig. 5C). Averaged normalized activation curves are shown in Fig. 5D (mean ± 95% CI). The

Fig. 5. Effect of Pyr9 ($50 \mu\text{mol l}^{-1}$) on the Na^+ current activation curve. (A) Peak Na^+ current plotted against test voltage (E_m). These curves were obtained from abdominal flexor motoneurons in five independent experiments by step depolarizations (5 ms; from -60 mV to 40 mV) from a holding potential of -70 mV in control conditions (filled symbols) and in the presence of $50 \mu\text{mol l}^{-1}$ Pyr9 (open symbols). Different symbols represent different motoneurons. All curves have been normalized to the maximum Na^+ current amplitude obtained under control conditions. (B) Averaged curves from A; all curves have been normalized to the maximum Na^+ current amplitude obtained for each curve. Vertical bars indicate 95 % confidence interval; $N=5$. (C) Chord conductance curves obtained from A (see text for explanation). All curves have been normalized to the maximum chord conductance obtained under control conditions. (D) Averaged activation curves obtained from C. All curves have been normalized (N_∞) to the maximum chord conductance obtained for each curve. Vertical bars indicate 95 % confidence interval; $N=5$.



smoothed curves are from the Boltzman equation, fitted to the data using a least-squares algorithm:

$$N_\infty = \frac{1}{1 + e^{(V_m - V_{50})/K}}, \quad (3)$$

where N_∞ is the relative activation parameter which, varies from zero to one as the chord conductance varies from zero to its maximum value (i.e. it is the normalized chord conductance), V_{50} is the half-activation potential, V_m is the test voltage and K is the slope factor. Under control conditions $V_{50} = -41.91 \pm 1.02 \text{ mV}$ and $K = 4.18 \pm 0.94$ ($r^2 = 0.94$); in the presence of Pyr9, $V_{50} = -43.14 \pm 0.71 \text{ mV}$ and $K = 3.18 \pm 0.63$ ($r^2 = 0.97$; mean \pm 95 % CI). No significant difference exists between these two activation curves (t -test, $P = 0.0748$ for V_{50} and $P = 0.102$ for K).

Neither the threshold voltage for the activation of Na^+ channels nor the reversal potential of the Na^+ current was affected by Pyr9. These results show not only that Pyr9 treatment has no effect on the voltage-dependence of Na^+ channel activation, but also that there is no drift over the period of the voltage recordings. This latter fact proves that the shift in the Na^+ inactivation curve towards more hyperpolarized potentials during Pyr9 treatment (see below) cannot be due to an artefactual deviation in the voltage recordings.

Effect of Pyr9 on the Na^+ current inactivation curve

To test the voltage-dependence of the tonic inhibition, we investigated the effects of Pyr9 on steady-state inactivation

(Fig. 6). The inactivation was assessed by the amplitude of the Na^+ current elicited by a test pulse to -30 mV after a prepulse to various potentials. In Fig. 6A,C,D, symbols plot the relative peak size of I_{Na} versus the potential of the prepulse, forming steady-state inactivation curves (H_∞ curves). The smooth curves are from the Boltzman equation fitted to the data using a least-squares algorithm:

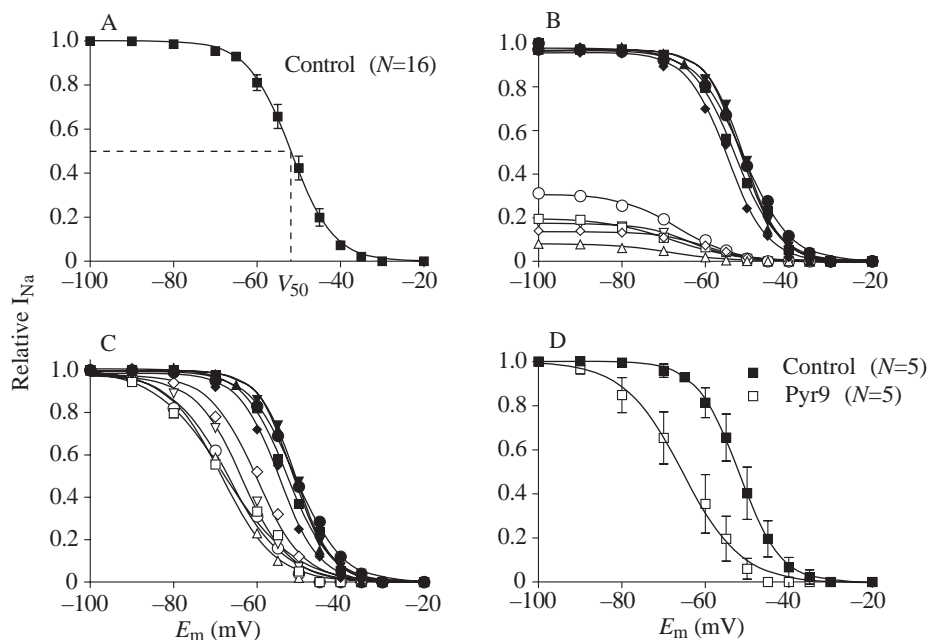
$$H_\infty = \frac{1}{1 + e^{(V_m - V_{50})/K}}, \quad (4)$$

where V_m is membrane potential, V_{50} is the prepulse potential for half-inactivation, and K is the slope factor. The Na^+ current inactivation curve obtained from 16 recordings from abdominal flexor motoneurone fibres is presented in Fig. 6A ($V_{50} = -51.90 \pm 0.33$; $K = 5.10 \pm 0.31$; mean \pm 95 % CI; $r^2 = 0.98$).

The effect of Pyr9 on the Na^+ current inactivation curve was studied in five experiments (Fig. 6B–D). I_{Na} was normalized either to the maximum peak amplitude obtained under control conditions (Fig. 6B) or to the maximum peak amplitude obtained for each curve (Fig. 6C,D). These data were obtained in the presence of external TEA^+ (10 mmol l^{-1}) and 4-AP (1 mmol l^{-1}). Various conditioning potentials, maintained for 500 ms, were used to obtain a slow Na^+ inactivation curve under control conditions (filled symbols) and after 40 min in the presence of $50 \mu\text{mol l}^{-1}$ of Pyr9 (open symbols). After Pyr9 application, the maximum peak amplitude of the Na^+ current was reduced by 67–92 % (Fig. 6B). In addition, in each experiment, the inactivation curve was shifted towards more

Fig. 6. Effects of Pyr9 (50 $\mu\text{mol l}^{-1}$) on the Na⁺ current inactivation curve.

(A) Normalized Na⁺ current inactivation curve from abdominal flexor motoneurons ($N=16$) (prepulse 500 ms to various potentials, E_m ; test pulse -30 mV, 5 ms). Between test pulses, the holding potential was maintained at -70 mV. Half-inactivation potential $V_{50}=-51.9$ mV. Vertical bars indicate 95 % confidence interval. (B) Effect of Pyr9 (open symbols) on the Na⁺ current inactivation curve ($N=5$); all curves have been normalized to the maximum Na⁺ current amplitude obtained under control conditions (filled symbols). Different symbols represent individual motoneurons. (C) Same data as in B with all the curves normalized to the maximum Na⁺ current amplitude obtained for each curve. Note that the inactivation curves obtained after 67 % (\circ), 80 % (\square) and 92 % (\triangle) inhibition by Pyr9 are very similar. This result indicates that the shift in the inactivation curve induced by Pyr9 was not the result of the residual current being modulated in a different manner to the totally inhibited current. (D) Averaged inactivation curves from the five experiments under control conditions (filled squares) and in the presence of Pyr9 (open squares). Vertical bars indicate 95 % confidence interval.



hyperpolarized potentials (Fig. 6C). The amplitude of the shift was not related to the degree of inhibition of the Na⁺ current by Pyr9 (Fig. 6C). Fig. 6D gives the mean values of the control data and the Pyr9 data. Under control conditions, there was no inactivation of the inward current at potentials below -80 mV and inactivation was 100 % for potentials above -35 mV. The smooth curve was fitted to the control data ($r^2=0.99$) using equation 4, with $V_{50}=-52.02\pm 0.49$ mV (95 % CI) and $K=4.95\pm 0.46$ (95 % CI). In the presence of Pyr9, there was no inactivation of the inward current at potentials below -100 mV and it was completely inactivated at potentials above -45 mV. The smooth curve was fitted to data in the presence of Pyr9 ($r^2=0.98$); the slope factor is significantly ($P<0.001$) higher ($K=7.14\pm 0.79$), whereas a significant ($P<0.001$) negative shift of -13.6 ± 1.5 mV in the half-inactivation potential is observed ($V_{50}=-65.70\pm 1.00$ mV). All values are given with 95 % confidence interval.

In two experiments, the state-dependence of the inhibition by Pyr9 was studied, using sustained conditioning potentials (duration greater than 5 min) to reach steady-state values of I_{Na} . In these two experiments, after 1 h in the presence of Pyr9, the Na⁺ current was reduced to 20 % and 8 % of its value under control conditions (Fig. 7A). When conditioning potentials were applied for long periods (more than 5 min), Na⁺ current amplitude reached a plateau in approximately 2 min for each conditioning potential value. The normalized inactivation curves obtained in the presence of Pyr9 using these two protocols (Fig. 7B) showed a decrease in the slope factor (4.5 and 5.8) for the steady-state protocol (2 min conditioning potentials) versus 8.2 and 6.2, respectively, for the slow protocol (500 ms conditioning potentials). The steady-state

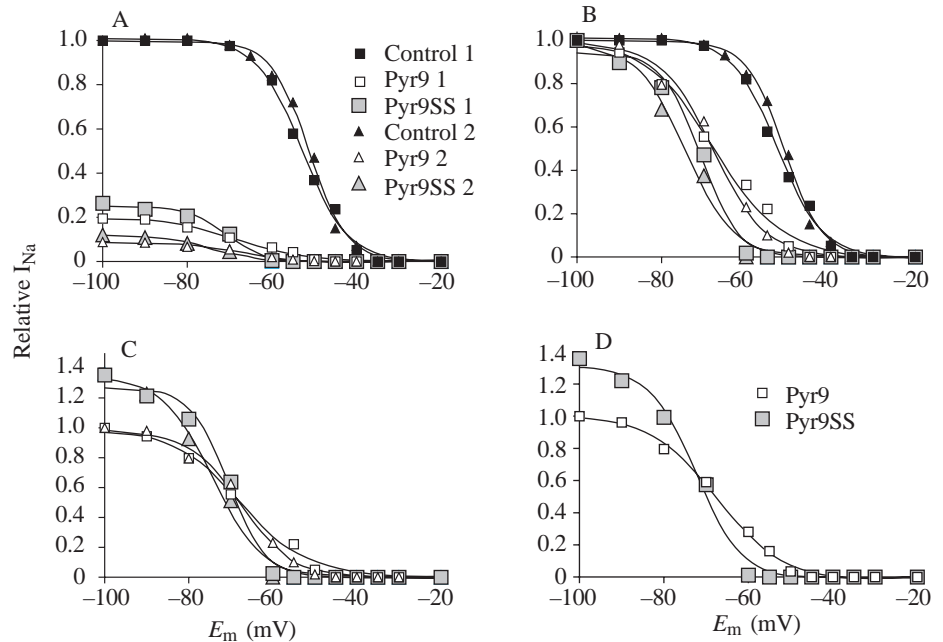
inactivation curves are shifted towards hyperpolarized potentials: $V_{50}=-70.8$ mV and -74.4 mV in the steady-state condition, whereas $V_{50}=-67.7$ mV and -67.6 mV in the slow condition. This change in the Na⁺ inactivation curve is due to a slight recovery at hyperpolarized potentials as well as a more pronounced block at depolarized potentials (Fig. 7C,D). The effect of Pyr9 on the Na⁺ current appears, therefore, to be state-dependent, the inhibition being more effective at depolarized membrane potentials (i.e. for the inactivated state).

The inactivation curves from abdominal depressor motoneurons obtained in the present study with a 500 ms prepulse duration (Fig. 6B) resemble the rapid rather than the slow Na⁺ current inactivation curves obtained by other authors from crayfish giant axon (Muramatsu *et al.* 1987; Salgado, 1992). We therefore used two different prepulse durations, short (30 ms) and long (500 ms), to give access to rapid and slow inactivations respectively. The Na⁺ current inactivation curves from abdominal flexor motoneurons obtained with long prepulses ($N=9$) are shown in Fig. 8, together with recordings obtained with short prepulses ($N=4$). It is noteworthy that most of the Na⁺ current is de-inactivated by short hyperpolarizing prepulses and that there is very little difference in the voltage-dependence of slow and rapid inactivation in any of the abdominal flexor motoneurons tested.

Discussion

The main question concerning the mechanism of action of Pyr9 on Na⁺ channels is whether this type of channel is the main target of the toxin. We obtained convergent results using

Fig. 7. Voltage-dependence of the inhibitory effect of Pyr9. (A) Slow Na^+ inactivation curves from two abdominal depressor motoneurons obtained with conditioning potentials (E_m) maintained for 500 ms under control conditions (filled symbols) and after 1 h in the presence of Pyr9 ($50 \mu\text{mol l}^{-1}$) (open symbols). The steady-state Na^+ current inactivation curves obtained with conditioning potentials maintained for 2 min after 1 h in the presence of Pyr9 (Pyr9SS) are also shown (shaded symbols). All data have been normalized to the maximum Na^+ current amplitude obtained under control conditions. (B) Same results shown in A normalized to the maximum Na^+ current amplitude obtained for each curve. (C) Data from A obtained in the presence of Pyr9 normalized to the maximum Na^+ current amplitude obtained with a 500 ms conditioning potential (open symbols; slow inactivation curve). A partial recovery (30–35% increase in the maximum Na^+ current amplitude) is observed when long-duration (>5 min) hyperpolarizing conditioning potentials were used (shaded symbols; steady-state inactivation curve). (D) Averaged inactivation curves presented in C in slow (open squares) and steady-state (shaded squares) conditions.



two types of *in vitro* nerve preparations to examine the blockade of nerve conduction, but this does not rule out other possible targets for Pyr9. *In vitro* experiments have shown that dialkylpyrrolidines inhibit acetylcholinesterase from *Torpedo torpedo*, but no inhibition could be observed on acetylcholinesterase from *Musca domestica* (Escoubas, 1988). This does not rule out a possible action on the postsynaptic receptor for acetylcholine, as demonstrated with the 1-methyl-5-alkyl-piperidines, structurally closely related toxins (Yeh *et al.* 1975; David *et al.* 1990). Conversely, could an inhibition of the Na^+ current explain the observed paralysis of insects after Pyr9 treatment? The problem with Na^+ current inhibition is that it has to be nearly complete to cause severe perturbation of nerve conduction. Pyr9 proves to be a weak inhibitor of the Na^+ channel, so that paralysis would result only at high doses. Nevertheless, the physicochemical characteristics of Pyr9 favour a high degree of accumulation of this toxin in hydrophobic tissues surrounding nerves. According to Gerolt (1969), lipophilic toxins typically applied on insect cuticle can reach nervous tissues directly through the hydrophobic tracheal system. Thus, in our experiments, the conduction blockade obtained after a 'topical' application of Pyr9 on a motor nerve through a hydrophobic interface (see Fig. 1) mimics what could happen after a topical application of ant venom on the cuticle of a termite. Nerve conduction blockade could be complete at such hydrophobic sites where toxins accumulate, thus impairing orthodromic spike conduction.

To study the mechanism of action of this nervous conduction blockade in more detail, we applied Pyr9 by external perfusion as an aqueous dispersion. The tonic inhibition developed under

conditions where the membrane potential was held at -70 mV and depolarizing pulses were applied infrequently. If we consider the 'rapid' inactivation curve obtained with a 30 ms prepulse and the 'slow' inactivation curve obtained with a 500 ms prepulse (see Figs 6–8), at a holding potential of

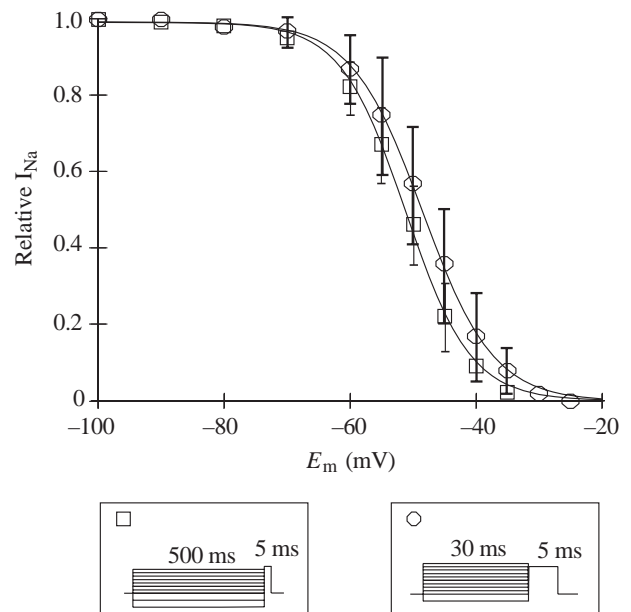


Fig. 8. Rapid Na^+ current inactivation curve (open circles, $N=4$) and slow Na^+ current inactivation curve (open squares, $N=9$) from abdominal flexor motoneurons. The protocols applied are shown in the insets. Data are presented as mean values \pm S.D.

-70 mV, most of the Na⁺ channels should be in the resting state. These results indicate that Pyr9 inhibits Na⁺ channels in their resting state. Nevertheless, the shift of the inactivation curve towards a more hyperpolarized potential indicates a preferential binding of the drug to the inactivated state of the channel (Salgado, 1992; Hille, 1977a,b; Bean *et al.* 1983; Hondghem and Katzung, 1984). The effect of Pyr9 on Na⁺ current inactivation curves in abdominal flexor motoneurons is very similar to the result obtained by Hille using myelinated axons from the sciatic nerve of the frog *Rana pipiens* treated with lidocaine (1 mmol l⁻¹). Hille (1977a,b) showed both a shift in the semi-inactivation potential in the hyperpolarizing direction and an augmentation of the slope factor of the curve. Even though it is not clear whether Pyr9 can bind to the Na⁺ channel in its resting state, our results do indicate that Pyr9 has a higher affinity for inactivated than for resting channels, as is the case for local anaesthetics, according to the modulated receptor model (Hille, 1977a,b; Hondghem and Katzung, 1984).

Hille (1977a,b) showed that the time constants for recovery from slow Na⁺ channel inactivation induced by different local anaesthetics strongly resemble the half-inhibition times characteristic for a sudden application of each drug. Thus, the recovery of local-anaesthetic-treated Na⁺ channels was observed in a matter of seconds in response to hyperpolarization. Whereas the neutral benzocaine could unblock rapidly from Na⁺ channels on hyperpolarization by a lipophilic route, local anaesthetics consisting of an ionisable amine showed slower recovery. More recently, Salgado (1992) pointed out the slow inhibitory action of dihydropyrazoles on Na⁺ currents and showed that Na⁺ channels treated with these insecticides could be unblocked only very slowly on hyperpolarization. In this study, the half-inhibition time characteristic for a sudden application of Pyr9 proved to be equivalent to that observed for dihydropyrazoles (Salgado, 1992), several orders of magnitude slower than that of local anaesthetics (Hille, 1977a,b). Because of our voltage-clamp configuration, it was difficult to maintain an axon at a hyperpolarized potential for a long time; nevertheless, partial recovery after Pyr9 treatment was observed with hyperpolarizations maintained for 2 min (Fig. 7D). A complete recovery should be observed only when hyperpolarization is maintained for much longer, taking into account the slow inhibiting effect of Pyr9 on Na⁺ current.

In addition to the tonic inhibition described above, Pyr9 application led to a phasic inhibition (40% inhibition at a concentration of 50 μmol l⁻¹, pH 7.6). Chernoff and Strichartz (1990) demonstrated a comparable phasic inhibition of Na⁺ channels by *d*-bupivacaine (40% inhibition at a concentration of 25 μmol l⁻¹, pH 7.3). In Courtney's (1975) model, the parameter Λ describes the accumulation of block during a test pulse (Chernoff, 1990). The values of Λ for *d*-bupivacaine (0.070 pulse⁻¹) are very close to Λ for Pyr9 (0.072 pulse⁻¹), indicating that the kinetic parameters of Pyr9 phasic inhibition are very similar to these of *d*-bupivacaine.

We are grateful to Professor G. Lhommet for supplying Pyr9. This work was supported by the Centre National de la Recherche Scientifique (CNRS).

References

- BEAN, B. P., COHEN, C. J. AND TSIEN, R. W. (1983). Lidocaine block of cardiac Na⁺ channels. *J. gen. Physiol.* **81**, 613–642.
- BLUM, M. S., BRAND, J. M., DUFIELD, R. M. AND SNELLING, R. R. (1973). Chemistry of the venom of *Solenopsis aurea*. *Ann. ent. Soc. Am.* **66**, 702.
- BLUM, M. S., JONES, T. H., LLOYD, H. A., FALES, H. M., SNELLING, R. R., LUBIN, Y. AND TORRES, J. (1985). Poison gland products of *Solenopsis* and *Monomorium* species. *J. ent. Sci.* **20**, 254–257.
- BLUM, M. S., ROBERTS, J. E. AND NOVAK, A. F. (1961). Chemical and biological characterization of venom of the ant *Solenopsis xyloni*. *Psyche* **68**, 73–74.
- BRAND, J. M., BLUM, M. S., FALES, H. M. AND MACCONNELL, J. G. (1972). Fire ant venoms: comparative analyses of alkaloidal components. *Toxicon* **10**, 259–271.
- CATTAERT, D. AND LEBRUN, B. (1993). A new configuration for voltage-clamp of axons used to demonstrate nerve conduction blockade by a 2,5-disubstituted pyrrolidine. *J. Neurosci. Meth.* **46**, 209–215.
- CHERNOFF, D. M. (1990). Kinetic analysis of phasic inhibition of neuronal Na⁺ currents by lidocaine and bupivacaine. *Biophys. J. biophys. Soc.* **58**, 53–68.
- CHERNOFF, D. M. AND STRICHARTZ, G. R. (1990). Kinetics of local anesthetic inhibition of neuronal Na⁺ currents: pH and hydrophobicity dependence. *Biophys. J. biophys. Soc.* **58**, 69–81.
- CLÉMENT, J. L., LEMAIRE, M., LANGE, C., LHOMMET, G., CÉLERIER, J. P., BASSELIER, J. J. AND CASSIER, P. (1985a). Insecticidal and/or acaricidal including termiticidal compositions based on 2,5-disubstituted derivatives of Pyrrolidine and/or Pyrroline 1. Brevet U.S. no. 727-057 25 avril.
- CLÉMENT, J. L., LEMAIRE, M., LANGE, C., LHOMMET, G., CÉLERIER, J. P., BASSELIER, J. J. AND CASSIER, P. (1985b). Compositions insecticides et/ou acaricides, notamment termiticides, à base de dérivés 2,5-disubstitués de la pyrrolidine et/ou de la pyrroline 1. Brevet européen no. 85-400866 1-3 mai.
- COURTNEY, K. R. (1975). Mechanism of frequency-dependent inhibition of Na⁺ currents in frog myelinated nerve by the lidocaine derivative GEA 968. *J. Pharmac. exp. Ther.* **195**, 225–236.
- DAVID, J. A., CROWLEY, P. J., HALL, S. G., BATTERSBY, M. AND SATELLE, D. B. (1990). Action of synthetic piperidine derivatives on an insect acetylcholine receptor/ion channel complex. *J. Insect Physiol.* **30**, 191–196.
- ESCOUBAS, P. (1988). Alcaloïdes de fourmis: identification, toxicité et mode d'action. Thèse, Université Paris VI, France.
- ESCOUBAS, P. AND BLUM, M. S. (1990). The biological activities of ant-derived alkaloids. In *Applied Myrmecology: A World Perspective* (ed. R. K. Van der Meer, K. Jaffe and A. Cedeno), pp. 483–489. New York: Westview Press.
- GEROLT, P. (1969). Mode of entry of contact insecticides. *J. Insect Physiol.* **15**, 563–580.
- GESSNER, W., TAKAHASHI, K. AND BROSSI, A. (1987). Synthesis of (±)-trans-2,5-dialkylpyrrolidines from the Lukes-Sorm Dilactam: efficient preparation of (±)-trans-2-butyl-5-heptylpyrrolidine and analogs present in ant venoms. *Helv. chim. Acta* **70**, 2003–2010.
- HILLE, B. (1977a). The pH-dependent rate of action of local anaesthetics on the node of Ranvier. *J. gen. Physiol.* **69**, 475–496.

- HILLE, B. (1977b). Local anesthetics: hydrophilic and hydrophobic pathways for the drug-receptor reaction. *J. gen. Physiol.* **69**, 497–515.
- HONDGHEM, L. M. AND KATZUNG, B. G. (1984). Antiarrhythmic agents: the modulated receptor mechanism of action Na⁺ and calcium channel-blocking drugs. *A. Rev. Pharmac. Toxicol.* **24**, 387–423.
- JONES, T. H. AND BLUM, M. S. (1983). Arthropod alkaloids: distribution, functions and chemistry. In *Alkaloids: Chemical and Biological Perspectives*, vol. 1 (ed. S. W. Pelletier), pp. 33–83. New York: John Wiley & Sons, Inc.
- JONES, T. H., BLUM, M. S., ANDERSEN, A. N., FALES, H. M. AND ESCOUBAS, P. (1988). Novel 2-ethyl-5-alkylpyrrolidines in the venom of an Australian ant of the genus *Monomorium*. *J. chem. Ecol.* **14**, 35–45.
- JONES, T. H., BLUM, M. S., HOWARD, R. W., MACDANIEL, C. A., FALES, H. M., DUBOIS, M. B. AND TORRES, J. (1982). Venom chemistry of ants in the genus *Monomorium*. *J. chem. Ecol.* **8**, 285–300.
- JONES, T. H., DE VRIES, P. J. AND ESCOUBAS, P. (1991). Chemistry of venom alkaloids in the ant *Megalomyrmex foreli* (Myrmicinae) from Costa Rica. *J. chem. Ecol.* **17**, 2507–2518.
- KUGLER, C. (1979). Evolution of the sting apparatus in the Myrmicinae ants. *Evolution* **33**, 117–130.
- MACCONNELL, J. G., BLUM, M. S. AND FALES, H. M. (1970). Alkaloid from fire ant venom: identification and synthesis. *Science* **168**, 840–844.
- MURAMATSU, I., NODA, M., NISHIO, M. AND FUJIWARA, M. (1987). Mechanism of Na⁺ channel block in crayfish giant axons by 711389-S, a new antiarrhythmic drug. *J. Pharmac. exp. Ther.* **242**, 269–276.
- PEDDER, D. J., FALES, H. M., JAOUNI, T., BLUM, M. S., MACCONNELL, J. G. AND CREWE, R. M. (1976). Constituents of the venom of a South African fire ant (*Solenopsis punctaticeps*), 2,5-dialkylpyrrolidines and pyrrolines: identification and synthesis. *Tetrahedron* **32**, 2275–2279.
- SALGADO, V. L. (1992). Slow voltage-dependent block of Na⁺ channels in crayfish nerve by dihydropyrazole insecticides. *Molec. Pharmac.* **41**, 120–126.
- SQALLI-HOUSSAINI, Y., CAZALET, J. R., FABRE, J. C. AND CLARAC, F. (1991). A cooling/heating system for the use with *in vitro* preparations: study of temperature effects on newborn rat rhythmic activities. *J. Neurosci. Meth.* **39**, 131–139.
- YEH, J. Z., NARAHASHI, T. AND ALMON, R. R. (1975). Characterisation of neuromuscular blocking action of piperidine derivatives. *J. Pharmac. exp. Ther.* **194**, 373–383.